Computer simulation of factors affecting drift from a forestry airblast sprayer

M.M. Sidahmed[1] and R.B. Brown[2]

[1]Department of Land and Water Resources, American University of Beirut, Beirut, Lebanon; and [2]School of Engineering, University of Guelph, Guelph, Ontario, Canada N1G 2W1.

Sidahmed, M.M. and Brown, R.B. 2002. **Computer simulation of factors affecting drift from a forestry airblast sprayer**. Canadian Biosystems Engineering/Le génie des biosystèmes au Canada **44**: 2.27-2.35. Previous studies have demonstrated the adequacy of the computational fluid dynamics code (FLUENT®) for simulating spray dispersal and deposition. In this study FLUENT® was used to determine the effects of weather and operating parameters on the behavior of droplets and consequences on drift and deposition with an airblast forestry sprayer (Algonquin®). The investigated parameters included initial droplet sizes (D_o=20-300 μm), temperature (T= 293 and 301 K), relative humidity (RH= 40, 69, and 80%), airblast outlet velocity (U = 30 and 48 m/s), and droplet projection angle (θ = 0, ±22.5, and ±45°). Temperature and RH had a pronounced influence on final droplet size, but had little effect on the horizontal distance traveled by droplets with D_o>70 μm. Conversely, U and θ had a significant effect on horizontal distance traveled by droplets with D_o>70 μm, but had little influence on final droplet size. Maximum possible swath ranged from 15 to 21 m for the variation of parameters investigated. Low RH caused excessive evaporation and should be avoided even at low temperature. High RH and low T conditions retarded evaporation while increasing both deposition within a spray swath and particle and airborne drift. High airjet speed and above-horizontal projection of droplets reduced deposition while increasing total particle and airborne drift. In all cases, drift would be drastically reduced by selecting nozzles that produce fewer small droplets (<110 μm) and orienting the nozzles downward (around –22.5°). **Keywords:** air-assisted spraying, airblast sprayers, forestry sprayers, drift simulation.

Des études ont démontré que le code informatique de dynamique des fluides (FLUENT) peut simuler adéquatement la dispersion et la déposition de jets pulvérisés. Dans la présente étude, FLUENT a été utilisé pour déterminer les effets de paramètres météorologiques et opérationnels sur le comportement des gouttelettes et les conséquences sur la dérive et la pulvérisation lors de l'utilisation d'un pulvérisateur à jet porté (Algonquin). Les paramètres étudiés incluaient la taille initiale des gouttelettes (D_o=20-300 μm), la température (T=293 et 301 K), l'humidité relative (HR=40, 69 et 80%), la vitesse à la sortie de la buse (U=30 et 48 m/s) et l'angle de projection des gouttelettes (θ = 0, ±22,5 et ±45°). La température et l'humidité relative ont eu un effet prononcé sur la taille finale des gouttelettes mais elles ont eu peu d'effet sur la distance horizontale parcourue par la gouttelette pour D_o>70 μm. À l'opposé, U et θ ont eu un effet significatif sur la distance horizontale parcourue par les gouttelettes pour D_o>70 μm, mais peu d'influence sur la taille finale des gouttelettes. La largeur d'épandage maximale possible a varié de 15 à 21 m pour l'ensemble des paramètres étudiés. Une HR faible a causé une perte par évaporation excessive et la pulvérisation dans de telles conditions devrait être évitée même si la température est basse. Une HR élevée et de faibles températures ont retardé l'évaporation tout en augmentant la déposition à l'intérieur du patron d'épandage et la dérive aérienne des particules. Une vitesse élevée de la vitesse du jet et un angle prononcé de projection des gouttelettes au dessus de l'horizontale ont réduit la déposition tout en augmentant la dérive aériennes des particules. Dans tous les cas, la dérive aurait été réduite de manière drastique en sélectionnant des buses qui produisent moins de petites gouttelettes (<110 μm) et en orientant les buses vers le bas (environ -22,5°). **Mots clés:** pulvérisation assistée à l'air, pulvérisateur à jet d'air, pulvérisateurs forestiers, simulation de dérive.

INTRODUCTION

Forestry herbicides are applied either by aircraft or by ground sprayers, which include boom, boomless (e.g. Boomjet and Boombuster), and airblast designs (Miller and Mitchell 1990; Desrochers and Dunnigan 1991). Airblast sprayers are considered superior for treating shelterwood sites where some trees are retained from harvest to provide the seed source and cover necessary for regeneration of the stand. The residual trees (i.e. not harvested mature trees) present problems for aerial applications as well as for ground applications with boom and boomless nozzles (Brown and Sidahmed 2001). Although effective for spraying shelterwood sites, airblast sprayers may create unacceptable spray drift with possible adverse effects on wildlife habitat and the fragile vegetative ecosystem.

To improve application efficiency and environmental safety, there is a need to establish proper spraying swath and buffer zone widths when spraying near environmentally sensitive areas. This requires proper understanding of the role and interaction of the factors that affect spray behavior. These factors include equipment parameters (nozzle type and size), application parameters (nozzle pressure or droplet size and nozzle orientation), weather parameters (temperature, relative humidity, and wind speed), and the physical properties of the spray liquid (surface tension, viscosity, and density). The effects of these parameters can be studied through field tests, wind tunnel experiments, and/or computer simulation. Both field tests and wind tunnel experiments are complicated, expensive, time consuming, and tedious. It is difficult, or impossible, to obtain the required weather conditions in field experiments. Normal sized wind tunnels cannot accommodate full airblast spraying systems (Legg and Miller 1990), and efforts to reproduce spray deposits from scale airblast sprayers in wind tunnels have not been very successful (Hale 1975, 1978). Therefore, computer simulation can be an invaluable tool for treating such problems.

Previous studies have demonstrated the adequacy of the computational fluid dynamics code FLUENT® (Fluent Inc., Lebanon, NH) to predict spray dispersal and deposition from

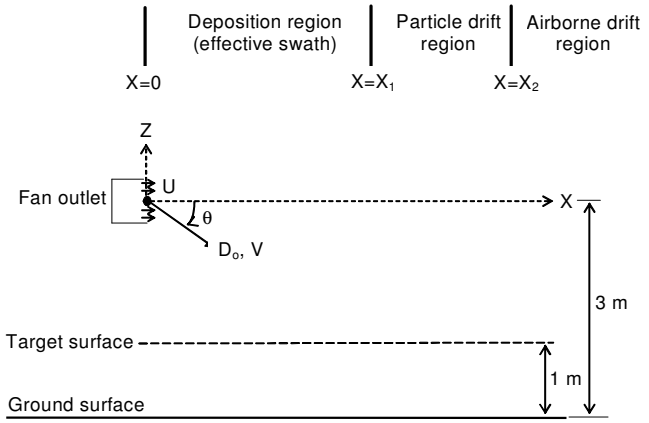

Fig. 1. Schematic showing the location of the airblast outlet relative to the ground and assumed target height; release of a droplet with initial diameter D_o and initial velocity V projected at an angle θ relative to the horizontal (θ is +ve counterclockwise) in an airblast with outlet velocity U; and the boundaries X_1 and X_2 which define the regions of spray deposition ($0<X<X_1$), particle-drift ($X_1<X<X_2$), and airborne drift ($X>X_2$).

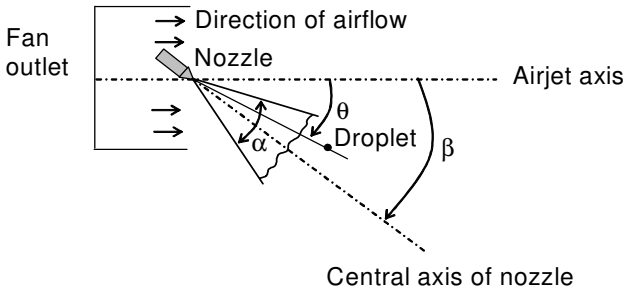

Fig. 2. Schematic showing the droplet projection angle θ ($\beta-\alpha/2\leq\theta\leq\beta+\alpha/2$) relative to the jet axis and central axis of a nozzle; α is the spray angle and β is the angle the central axis of the nozzle makes with the jet axis (both θ and β are +ve counter-clockwise).

airblast sprayers (Sidahmed and Brown 2001; Brown and Sidahmed, 2001). FLUENT® has also been verified for simulating spray drift in a wind tunnel (Reichard et al. 1992a, 1992b) and used to simulate drift of discrete water droplets from field sprayers (Zhu et al. 1994), study collection efficiency of spray droplets on vertical targets (Zhu et al. 1996), and to predict droplet dispersion from an orchard mistblower (Weiner and Parkin 1993). Previous studies, however, did not consider the effects of weather and application parameters on drift and deposition from forestry airblast sprayers.

In this study, FLUENT® was used to predict the effects of some of the principal parameters (droplet size, droplet release velocity and projection angle, airblast outlet velocity, temperature, and relative humidity) affecting the behavior of spray droplets in an airblast spray swath, and their consequences on drift and deposition.

MATERIALS and METHODS

System description

Evaluation of FLUENT® for simulation of the airflow field and droplet trajectories from the Algonquin® forestry airblast sprayer (manufactured by M.K. Rittenhouse & Sons, St. Catharines, ON) was discussed previously by Sidahmed and Brown (2001) and Brown and Sidahmed (2001). These papers also included a detailed description of the sprayer and the simulation equations of FLUENT®. Sidahmed and Brown (2001) verified the accuracy of FLUENT® for simulating round jets, which are characteristic of forestry airblast sprayers, using data collected from a small centrifugal fan and the Algonquin® airblast sprayer. Brown and Sidahmed (2001) conducted field experiments in a shelterwood forestry site using a tracer dye and artificial targets to evaluate the adequacy of FLUENT® in modeling droplet dispersion and deposition from the same sprayer. FLUENT® satisfactorily predicted the measured spray dispersion data from the sprayer but there were some discrepancies for smaller droplets (<47 μm). These droplets were predicted as depositing beyond 18 m from the sprayer outlet, while experimental data showed their presence within a range of 3 to 21 m. The discrepancy (or detection of <47 μm droplets closer to the sprayer outlet in the experimental data) was attributed to shattering of droplets upon impaction with targets, a process which FLUENT® cannot account for in the simulation.

The Algonquin® airblast sprayer uses a centrifugal blower, which produces a mean axial air velocity of 30 m/s from a 203 mm-diameter outlet located 3 m above the ground (Fig. 1). Three equally spaced cone nozzles (D2-25, RD1.5-23, and D2-23, Spraying Systems Co., Wheaton, IL) are mounted along the vertical axis of the outlet and are oriented horizontally so as to spray in the same direction as the airflow. The computational code employs the finite difference method for establishing the airflow field and tracking droplets. The airjet flow field is solved using Navier-Stokes equations for mass and momentum conservation and the standard two-equation k-ϵ turbulence model. Droplet trajectories are calculated by considering evaporation and solving the equation of motion of a droplet in a Lagrangian frame in Cartesian coordinates (X, Y, Z).

Simulation of factors affecting drift

The simulated droplet initial size range was from 20 to 300 μm diameter. The spray-application parameters included two initial droplet velocities (V = 20 and 45 m/s), two airblast velocities (U = 30 and 48 m/s), and five droplet projection angles (θ = 0, ±22.5, ±45°). The airjet was directed horizontally outward, and θ (positive counterclockwise) was the initial release angle of droplets from the nozzle (Fig. 2). As seen in Fig. 2, for a nozzle whose spray angle is α and whose central axis is at an angle β from the horizontal jet axis, the angle θ ranges from β-α/2 to β+α/2, where both θ and β are positive counterclock-wise. However, all simulations were performed assuming α=0 and β ranged from –45 to 45°.

Liquid was assumed to be pure water, and therefore the droplet diameter was directly related to the net amount of evaporation occurring while the droplet was airborne. The investigated weather parameters were combinations of two air temperatures (T = 293 and 301 K) and two relative humidities

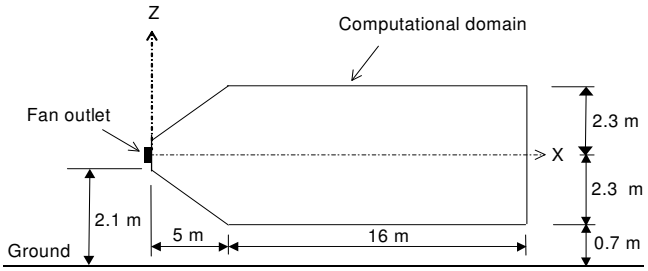

Fig. 3. Position of the computational domain (4.6 m × 4.6 m × 21 m long) relative to the ground (Brown and Sidahmed 2001).

(RH = 40 and 80%). The weather conditions (T=301 K and RH=69%) encountered in the field experiments of Brown and Sidahmed (2001) were also considered. Natural wind effects were not investigated, and therefore turbulence intensity of ambient air was assumed low, 7-10%. Areas under a forest cover, which is the case in shelterwood sites, benefit from being sheltered from the wind (Desrochers and Dunnigan 1991). Observations by Brown and Sidahmed (2001) during several days of field experiments confirmed the stillness of air within a shelterwood site.

The computational domain (Fig. 3) was the same as that described by Brown and Sidahmed (2001). It was 4.6 m × 4.6 m and extended 21 m from the airblast outlet of the stationary sprayer. All droplets were released from a 3 m height, which is the height of the airblast outlet. Simulations were performed assuming that the target or vegetation canopy was 1 m high, which was the case during the field experiments, and that droplets are not intercepted in transit by plants taller than 1 m.

The protocol used for computation of trajectories was the same for all simulated conditions. When a droplet with initial diameter D_o was released from the airblast outlet, FLUENT® calculated the diameter (D) and its coordinates (X, Y, Z) during flight (Fig. 1). The focus of the investigation was on D, X (which is the mean horizontal distance), and Z (which gives the height, H, of the droplet above the ground H = 3+Z). Trajectory calculations were terminated when one of the following conditions was satisfied: (1) the droplet had reached the target level (H =1 m), (2) the droplet had evaporated to extinction (D≈0) before reaching the target within 21 m from the sprayer outlet, or, (3) the droplet had escaped from the computational domain. The variables D_f (final diameter), L_f (final distance), and H_f (final height), respectively, denote the values of D, X, and H when trajectory calculations are terminated, and represent the mean values of multiple injections (or release into the airjet stream) of at least five droplets for each size.

RESULTS and DISCUSSION

The simulation results were examined in two ways. One analysis focused on determining how the various simulated weather and operating conditions affected the final distance, final height, and final diameter of spray droplets. The second analysis compared the theoretical performance of the sprayer with regard to deposition and drift under the various simulated conditions by identifying and comparing the predicted range of sizes of droplets that fell in the deposition, particle drift (ASAE 2002) and airborne drift (ASAE 2002) regions (Fig. 1). Actual amounts of drift and deposition were not calculated, since the droplet size distribution at the outlet of the sprayer was not measured due to lack of a suitable spray-sampling instrument.

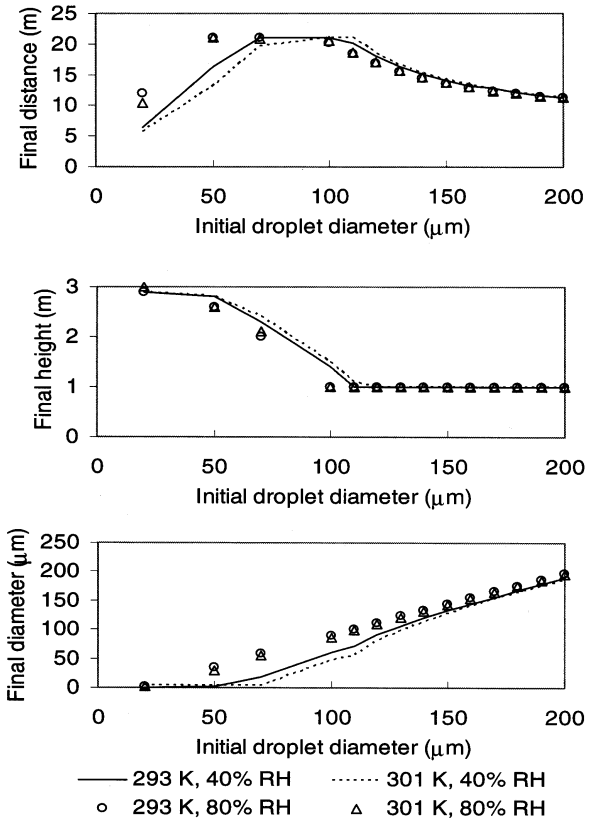

Fig. 4. Final distance, final height, and final diameter of droplet versus initial droplet diameter for different combinations of temperature and relative humidity. The droplets were released horizontally from a 3 m height above the ground with 45 m/s, assuming airjet speed = 30 m/s.

Trajectory data

Effects of air temperature and relative humidity Figure 4 shows the final distances (L_f), final heights (H_f), and final diameters (D_f) for droplets ranging from 20 to 200 μm initially, for a combination of two temperatures (293 and 301 K) and two relative humidities (40 and 80%). The droplets were projected horizontally (i.e. $\theta=0^o$) into the airblast stream with a 45 m/s initial velocity.

For all combinations of temperature and relative humidity in Fig. 4, the final distances traveled by large droplets (>120 μm) to reach the target (1 m above ground) were almost the same. For example, the final distance traveled by a 150 μm droplet to reach the target level was 14 m for 293 K and 40% RH, 14.2 m for 301 K and 40% RH, 13.6 m for 293 K and 80% RH, and 13.7 m for 301 K and 80% RH (the range was from 13.6 m to 14.2 m and represents a maximum variation of 4.4%). In general, the final distance traveled by droplets larger than 70 μm to fall to a given elevation was not greatly affected by changes in either temperature or relative humidity, or both.

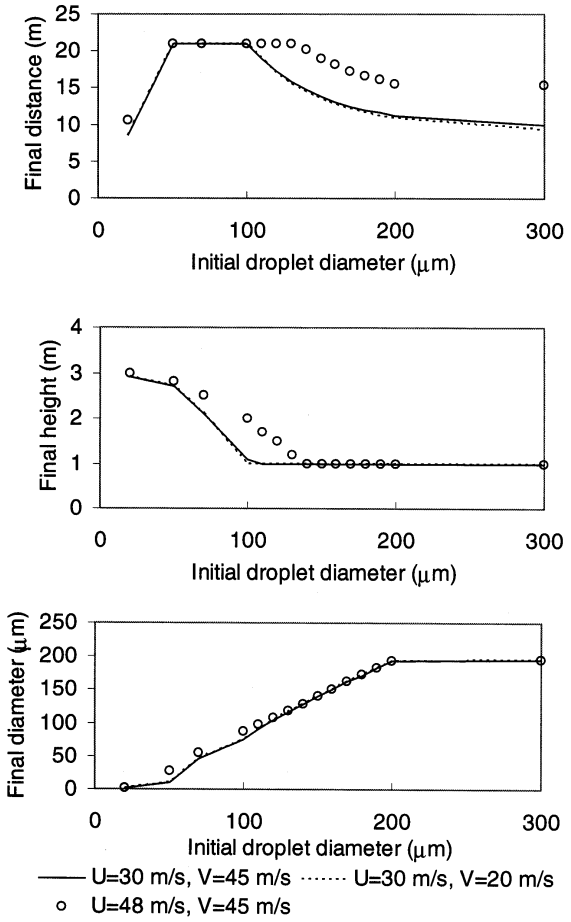

Fig. 5. Final distance, final height, and final diameter of droplet versus initial droplet diameter for different combinations of initial drop velocity V and airjet velocity U. The droplets were released horizontally from a 3 m height above the ground, assuming air temperature = 301 K and relative humidity = 69%.

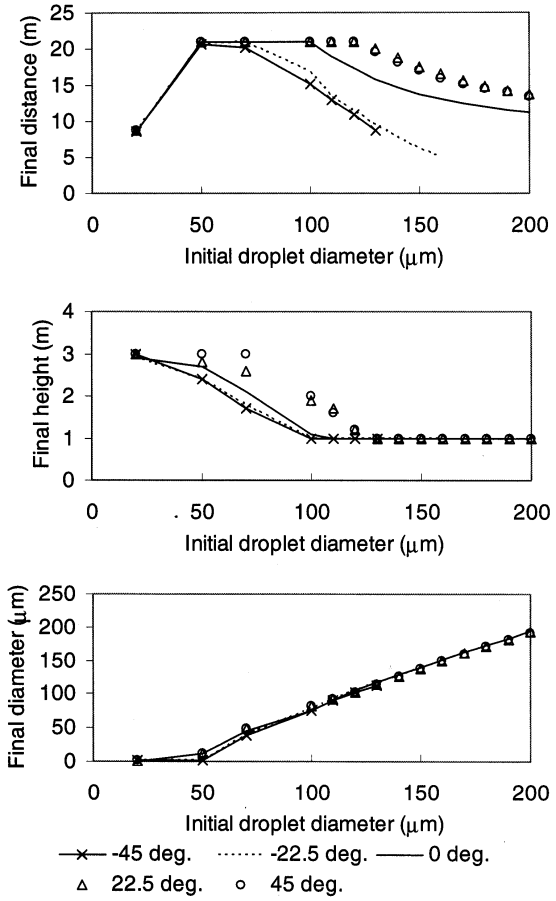

Fig. 6. Final distance, final height, and final diameter of droplet versus initial droplet diameter for different droplet projection angles (0°, ±22.5°, ±45°, +ve denotes above horizontal). The droplets were released from a 3 m height above the ground with 45 m/s, assuming airjet speed = 30 m/s, air temperature = 301 K and relative humidity = 69%.

At low humidity (40% RH), the final diameters were smaller at 301 K than at 293 K, and this difference was greater for the smaller droplet sizes (Fig. 4). As surface area-to-volume ratio increases greatly with decreasing droplet diameter, small droplets are much more affected by evaporation than are large droplets over the same trajectory. For example, at 40% RH, the final diameter of a 150 μm droplet was 133 μm (11% less) at 293 K, and 128 μm (15% less) at 301 K, while at 80% RH the final diameter was 145 μm (3% less) at 293 K and 143 μm (5% less) at 301 K. Thus, the effect of temperature on evaporation was more pronounced at low relative humidities. The worst case, as expected, was the condition where both high temperature and low relative humidity prevailed (40% RH and 301 K in Fig. 4).

Effects of initial velocity of droplets and airjet Figure 5 shows the final distances (L_f), final heights (H_f), and final diameters (D_f) for droplets of different initial sizes (20 to 300 μm), for different combinations of droplet-release and airjet velocities. The droplets were projected horizontally in all cases, assuming the temperature (301 K) and relative humidity (69%) encountered in the field experiment of Brown and Sidahmed (2001). First, current normal operating conditions of the sprayer were used (i.e. 30 m/s axial velocity and 45 m/s initial droplet-velocity). In the second case, the same airjet velocity was maintained (30 m/s axial velocity), while the initial droplet-velocity was reduced to 20 m/s. In the third case, the initial droplet velocity was 45 m/s and the airjet velocity was increased by 60% (from 30 to 48 m/s).

As seen in Fig. 5, reducing the initial velocity of droplets from 45 to 20 m/s had no significant effect on either final distance or final diameter of droplets. This indicates that droplets projected horizontally acquire the airjet velocity soon after their release, regardless of their initial velocity. On the other hand, increasing the airjet exit velocity for a constant initial droplet velocity significantly increased the final distances traveled by the droplets, while it had little effect on their final diameters. For example, the distance traveled by a 150 μm to fall to 1 m elevation was 13.8 m for the 30 m/s airjet speed and 19 m (38% more) for 48 m/s, while the final diameter in both cases was 140 μm.

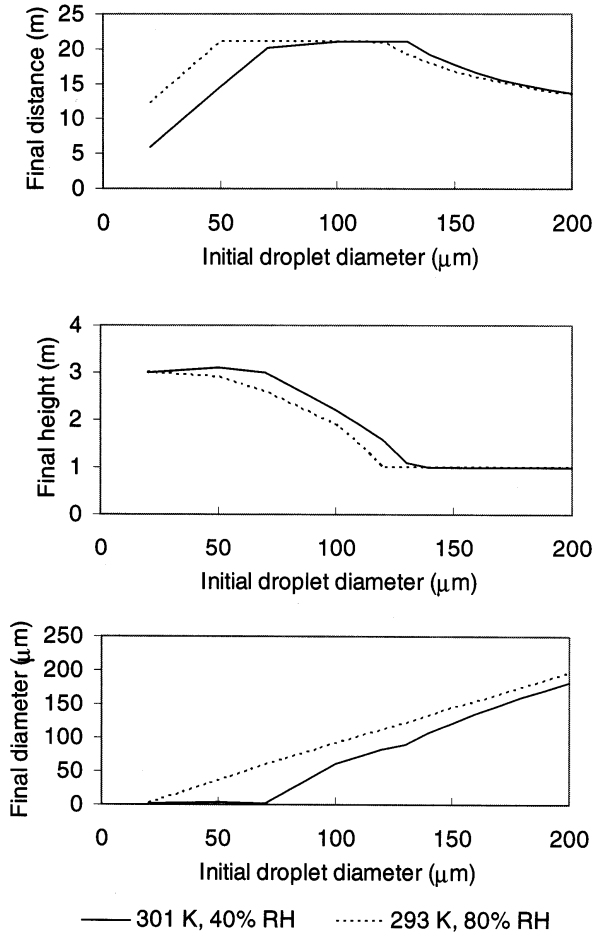

Fig. 7. Final distance, final height, and final diameter of droplet versus initial droplet diameter for two extreme cases of weather conditions representing hot dry (301 K and 40% RH) and cool damp (293 K and 80% RH). The droplets were released from a 3 m height above the ground at 45 m/s and 45° above-horizontal assuming airjet speed of 30 m/s.

Effects of droplet size and projection angle Figure 6 shows the final distances (L_f), final heights (H_f), and final diameters (D_f) for different initial droplet sizes (20-200 μm) and projection angles (0, ±22.5, and ±45°). Droplets were released with a velocity of 45 m/s assuming T= 301 K and RH = 69%. Note that, in Fig. 6, the final distance curves for below-horizontal projections are truncated at larger droplets (D_o > 140 μm for θ=-45°, and D_o > 170 μm for θ=-22.5°), because these droplets escaped from the lower boundary of the computational domain in the region 0 to 5 m from the outlet. For these droplets L_f was considered less than 5 m and D_f was not calculated.

The final distance that a given droplet traveled to fall to a given elevation varied with both its initial size and angle of projection from nozzle, but the final diameter was not sensitive to droplet projection angle (Fig. 6). The final distance was longest for above horizontal projections and shortest for below horizontal, while final distance for horizontal projection was intermediate between the two extremes. For example, the distance traveled by a 150 μm droplet to fall to 1 m elevation was 13.8 m for 0°, 6.3 m (54% less) for –22.5°, and 17.5 m (27% more) for 22.5° (percentages calculated relative to distance traveled at 0°), while the final diameters for all the projection angles ranged from 138 to 140 μm, which represents a maximum variation of 1.4%.

Effect of droplet projection angle, T, and RH Figure 7 shows the effect of above-horizontal projection angles under two extreme weather conditions, hot and dry (40% RH and 301 K) and cool and damp (80% RH and 293 K). The droplets were projected at 45° above the horizontal with 45 m/s initial velocity. Figures 7 and 4 are for the same droplet sizes and weather conditions, but different projection angles (45° and 0°). As seen in Figures 7 and 4, above-horizontal projection angles had almost the same effect for the two extreme weather conditions. The final distances were much longer at 45° than at 0°, but the final diameters were not significantly different, regardless of weather conditions. For example, at 301 K and 40% RH, the distance traveled by a 150 μm droplet was 14.2 m for 0° and 17.8 m (25% more) for 45°, while the final diameter was 133 μm for 0° and 128 μm (4% less) for 45°. Similarly, at 293 K and 80% RH, the distance traveled by a 150 μm droplet was 13.6 m for 0° and 16.7 m (23% more) for 45°, while the final diameter was 145 μm for 0° and 144 μm (0.1% less) for 45°.

Deposition and drift

Data in Figs. 4 to 7 were used to identify and compare the size ranges of droplets that fell in the deposition and drift regions, as illustrated in Fig. 8 and summarized in Table 1. The boundary X_1 was defined assuming the actual effective swath used by sprayer operators (i.e. X_1=14 m); it is worthwhile to mention that the 14 m is the horizontal distance (from the airblast outlet) where theoretically the airjet starts to impinge on the ground [see Eq. 8 in Sidahmed and Brown (2001)]. The boundary X_2 was estimated for each combination of weather and operating parameters as the distance beyond which droplets remain at an elevation above the estimated target level of 1 m. For each case in Figs. 4 to 7, X_2 was considered the L_f value at which H_f starts to exceed unity as explained in Fig. 8. As seen in Table 1, X_2 ranged from 19 to 21 m for all cases, except for the below horizontal projection angles where X_2 was around 15-17 m. In general, X_2 is constant for given weather and operating parameters, while X_1 is the swath width, which can be chosen independently by the sprayer operator. As effective swath increases, deposition increases and particle-drift decreases, and vice versa. The maximum possible swath is achieved when X_1=X_2, which is the case when particle drift is zero and only airborne and vapor drift occur (Fig. 8). Thus, X_2 also represents the maximum possible swath, and ranged from 15 to 21 m (Table 1).

The variables D_{o1} and D_{f1} (in Fig. 8 and Table 1) are the initial and final diameters of the largest droplet that crossed the boundary X_1 (i.e. largest droplet liable to drift). Likewise, D_{o2} and D_{f2} are the initial and final diameters of the largest droplet that crossed the boundary X_2 (i.e. largest droplet liable to remain airborne). The variable D_{oe} is the diameter of the largest droplet that evaporated to extinction. Thus, deposition would result from all droplets (or volume in droplets) with D_o>D_{o1} (or

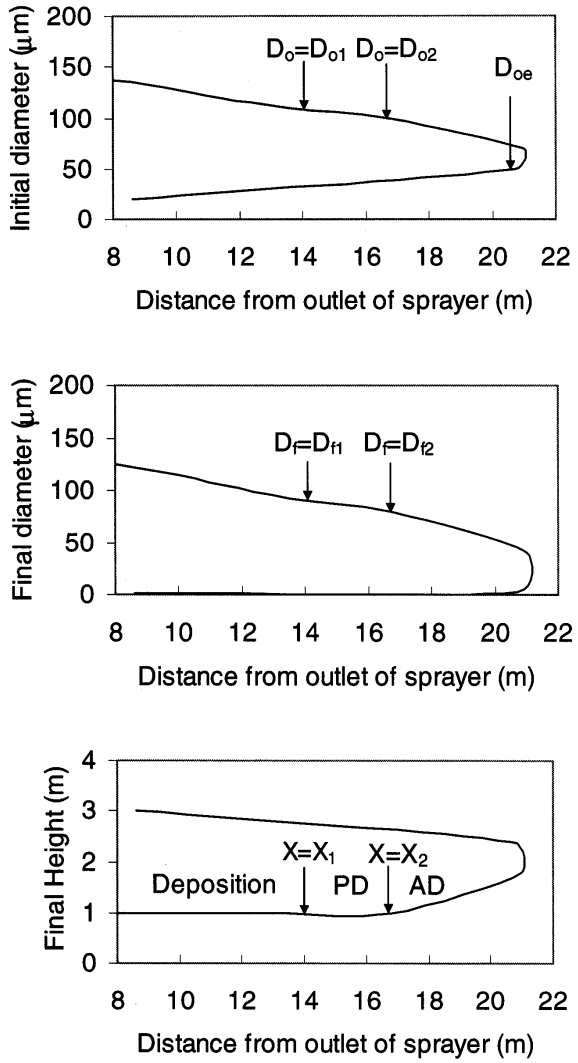

Fig. 8. Boundaries X_1 and X_2 and their corresponding droplet initial (D_o) and final (D_f) diameters that define the deposition, particle drift (PD), and airborne drift (AD) regions. Droplets were projected below horizontal at -22.5° and 45 m/s from a 3 m height, assuming airjet speed = 30 m/s, air temperature = 301K, relative humidity = 69%, and height of target = 1 m.

$D_f>D_{fl}$), particle drift was droplets with $D_{o2}<D_o<D_{o1}$, airborne drift was droplets with $D_{oe}<D_o<D_{o2}$, and vapor drift was the volume representing net evaporation while droplets were airborne i.e. difference between initial and final volume of the spray (Recall that the liquid was assumed to be pure water).

However, in absence of knowledge about droplet size distribution at the sprayer outlet, which was the case in this study, comparison of two spray volumes containing different size ranges is only possible if one range is a subset of the other. For example, for a given droplet size distribution the total volume of all droplets larger than, say 150 µm, must be greater than the volume contained in droplets larger than 180 µm, since the latter range is a subset of the former. Likewise, the total volume in droplets smaller than 150 µm is less than that in droplets smaller than 180 µm since the first range is a subset of the second range. It is not possible to compare the volume contained, for example, in droplets with 100<D<150 µm with that contained in droplets with 110<D<160 µm if the number of droplets in each size range (or droplet size distribution) is unknown, because neither range is a subset of the other. Therefore, for any two cases in Table 1, it was always possible to compare deposition and (in most cases) airborne drift separately, but not particle drift, which is bounded by D_{o1} and D_{o2}. Therefore, in most cases comparison of drift was based on total (or combined) particle and airborne drift, which is droplets with $D_{oe}<D_o<D_{o1}$ (Fig. 8 and Table 1).

Effect of airjet speed Since changing airjet speed (U) had no significant effect on final diameters (Fig. 5), then for a given initial droplet size distribution the final size distribution for 30 m/s airjet speed would be the same as that for 48 m/s. This also means that comparison of deposition and drift can be based on either initial or final diameters, but initial diameters were used to provide a common reference for comparison. As seen in Table 1 (cases 5 and 7), deposition for 48 m/s (D_o>273 µm) was lower than for 30 m/s (D_o>148 µm), but total particle and airborne drift for 48 m/s was higher than that for 30 m/s. The results also show that airborne drift alone for 48 m/s was higher than for 30 m/s. Thus, increasing airjet speed reduced deposition but also increased total particle and airborne drift.

Increasing airjet speed for a given swath width reduced the effective application rate (L/ha) because droplets traveled longer distances without significant reduction in their final diameters (i.e. same total volume more widely dispersed). For example, as mentioned earlier, for the 30 m/s axial velocity, a 150 µm droplet traveled 13.8 m before falling to a 1 m elevation, while for 48 m/s axial velocity the same droplet traveled 19 m (38% more) before falling to the same elevation (Fig. 5). The final diameter in both cases was 140 µm. This means that the final volume (contained in all drops with D_f>140 µm) applied over 13.8 m at 30 m/s is the same as that applied over 19 m at 48 m/s. Thus, increasing airjet speed from 30 to 48 m/s caused an effective reduction of 27% in the application rate (L/ha). Since final diameters (or evaporation) were the same for both jet speeds, then it is the difference in application rate that was converted into high particle and airborne drift.

Effect of droplet projection angle The effect of increasing droplet projection angle on deposition and drift was similar to that of increasing airjet speed, since both U and θ increased the final distances traveled by droplets and had little effect on final diameters. This means that increasing θ also caused an effective reduction in application rate, and consequently reduced deposition and promoted high particle and airborne drift. For example (cases 12, 10, and 8 in Table 1), deposition for 45° (D_o>190 µm) was less than for 0° (D_o>148 µm), which in turn was less than deposition for –45° (D_o>105 µm). Total particle and airborne drift for 45° was higher than that for 0°, which in turn was higher than that for -45°. The results also show that airborne drift alone for 45° was higher than for 0°, which in turn was higher than for –45°.

Thus, total particle and airborne drift was highest for above horizontal projection and lowest for below horizontal projection. Horizontal projection was intermediate between these two extremes. Having this, and since deposition for –22.5° (D_o>

Table 1. Initial (D_o) and final (D_f) diameters of droplets corresponding to the boundaries (X_1 and X_2) defining the deposition[a] region($0<X<X_1$), particle-drift[b] region ($X_1<X<X_2$), and airborne drift[c] region ($X>X_2$) for the different conditions simulated in Figs. 4 to 7.

Source of data	Case No.	Simulated conditions					At boundary $X^*=X_1$			At boundary $X=X_2$			At extinction
		RH (%)	T (K)	θ (°)	V (m/s)	U (m/s)	X_1 (m)	D_{o1} (μm)	D_{f1} (μm)	X_2 (m)	D_{o2} (μm)	D_{f2} (μm)	D_{oe} (μm)
Fig. 4	1	40	293	0	45	30	14	150	133	20	110	71	50
	2	40	301	0	45	30	14	152	131	19	120	80	70
	3	80	293	0	45	30	14	145	140	20	100	89	20
	4	80	301	0	45	30	14	147	139	21	100	85	20
Fig. 5	5	69	301	0	45	30	14	148	138	19	110	91	20
	6	69	301	0	20	30	14	145	135	21	100	76	20
	7	69	301	0	45	48	14	273	268	20	140	129	20
Fig. 6	8	69	301	-45	45	30	14	105	84	15	100	76	50
	9	69	301	-22.5	45	30	14	108	90	17	100	79	50
	10	69	301	0	45	30	14	148	138	19	110	91	20
	11	69	301	22.5	45	30	14	194	186	20	130	114	20
	12	69	301	45	45	30	14	190	182	20	130	114	20
Fig. 7	13	40	301	45	45	30	14	194	178	19	140	107	70
	14	80	293	45	45	30	14	187	179	21	120	110	20

[a] Deposition = volume of spray contained in drops with $D_o>D_{o1}$ (or $D_f>D_{f1}$)
[b] Particle drift = volume of spray contained in drops with $D_{o2}<D_o<D_{o1}$ (or $D_{f2}<D_f<D_{f1}$)
[c] Airborne drift = volume of spray contained in drops with $D_{oe}<D_o<D_{o2}$ (or $0<D_f<D_{f2}$)
*X = distance from fan outlet; D_{o1}, D_{f1} = respectively D_o, D_f of largest droplet that crossed boundary $X = X_1$; D_{o2}, D_{f2} = respectively D_o, D_f of largest droplet that crossed boundary $X = X_2$; D_{oe} = largest droplet that evaporated to extinction; RH = relative humidity; T = ambient air temperature; θ = droplet projection angle from horizontal; V = droplet release velocity; U = airjet velocity

108 μm) was comparable to that for –45° (D_o>105 μm), total particle and airborne drift can be drastically reduced if the selected nozzles produced fewer small droplets (<110 μm) and were oriented downward at –22.5°. With this orientation (β = -22.5°) and a spray angle of 45° (α=45°), the range of droplet projection angle for the spray would be $-45°<\theta<0°$ (see Fig. 2).

Effect of T and RH Unlike U and θ, T and RH had significant effect on final diameters (or evaporation) of droplets, and therefore a given droplet size distribution at the outlet of the sprayer can produce quite different final volume distributions, depending on differences in simulated weather conditions. Therefore care must be taken in using the inequality signs (> or <) when comparing drift and deposition using droplet size ranges. For example (cases 2 and 4 in Table 1), deposition for 301 K and 40% RH (D_o>152 μm) was less than for the same T and 80% RH (D_o>147 μm), since the range D_o>152 μm is a subset of the range D_o>147 μm, and since the final diameters of all droplets were much smaller at 40% RH than at 80% RH because of evaporation. Unlike the case with U and θ, this does not automatically mean that the spray volume in the range D_o<152 μm is less than that in the range D_o<147 μm, even though the latter range is a subset of the former, because of difference in evaporation.

As mentioned earlier, since the distance traveled by droplets larger than 70 μm was not significantly affected by RH (Fig. 4), then a droplet in any initial size range greater than 70 μm fell into the same region (deposition, particle drift, and airborne drift) whether the RH was 40 or 80%. However, since the final diameters of all droplets are much larger at 80% RH than at 40% (Fig. 4), then increasing RH increased deposition as well as particle drift and airborne drift. This means, as RH increased (at the same T) from 40 to 80%, not all the spray volume gained (due to reduction in evaporation) was converted into deposition, since a portion of this gain contributed to higher particle and airborne drift. We have confirmed this by applying the data of Table 1 to the USDA (1984) wind tunnel spray spectra (results not shown here). The USDA (1984) data were measured for the same size and type of nozzles (D2-23 and D2-25), orientation (nozzles spraying in same direction of airflow), and average air speed (23-45 m/s) as that of the airblast sprayer.

Thus, low relative humidity caused excessive evaporation, and consequently low deposition as well as low particle and airborne drift. Conversely, high relative humidity conditions retarded evaporation, and consequently caused high deposition as well as high particle-drift and airborne drift. Low relative humidity conditions should be avoided even at low temperatures. Also, when RH is very high, it is likely that high particle drift from adjacent passes of a sprayer can result in higher deposits in the overlap regions. This also represents an undesired environmental load.

Effect of droplet projection angle, T, and RH At a given T and RH, θ had little influence on the final diameter (or evaporation) of droplets (Fig. 6). Therefore, deposition and drift can be compared based on either initial or final diameter. Above-horizontal projection of droplets reduces deposition and increases total particle and airborne drift, regardless of the weather conditions. For example (cases 2 and 13 in Table 1), at 301 K and 40% RH, deposition for 0° (D_o>152 μm) was higher

than for 45° (D_o>194 μm). Total particle and airborne drift for 0° was lower than for 45°. Also, airborne drift alone for 0° was lower than for 45°. The results were similar when comparing 0 and 45° projection angles at different T and RH (293 K and 80% RH, cases 3 and 14 in Table 1). The effect of angle of projection was expected to be more significant at higher airjet velocities, particularly at low RH, since both high airjet velocity and low RH conditions also promote high particle and airborne drift.

The spray nozzles on the blower of the Algonquin sprayer are normally positioned horizontally (i.e. β=0). Above-horizontal projection of droplets can result from fanning of the spray liquid as it emerges from the nozzle. In this study, the effect of the airblast on the fan angle of the spray was not determined experimentally. However, above-horizontal projection angles can also result from bouncing and tilting of the sprayer due to uneven terrain. Orienting the spray nozzles downward as explained earlier would also minimize drift that would have otherwise been excessive at times when the airjet is directed above horizontal due to bouncing and tilting of the sprayer in rough terrain.

CONCLUSIONS

The following conclusions can be made from this study:

1. Airjet velocity and droplet projection angle affect drift by altering horizontal distance traveled by droplets with little effect on droplet size, while T and RH influence drift by affecting droplet size with little effect on traveled distance.
2. High temperature-low humidity conditions cause excessive evaporation and low deposition and should be avoided. Cool and damp conditions increase total deposition but also promote high particle and airborne drift.
3. The initial velocity of droplets projected horizontally from the nozzle had no effect on droplet trajectories or final diameters of droplets.
4. Selecting nozzles that produce fewer small droplets (<110 μm) and orienting the nozzles downward (around –22.5°) would drastically reduce drift. This nozzle orientation would also minimize drift that would have otherwise been excessive at times when the airblast is directed upward due to bouncing or tilting of the sprayer in rough terrain.

Simulation data of this study are useful to understand how spraying parameters should be adjusted to achieve a desired result, and to compare expected theoretical performance of the sprayer with regard to deposition and drift under various weather and operating conditions. They can also be used to calculate actual amount of drift and deposition if the droplet size spectra at the sprayer outlet is known. The results of this study can be used as baseline information that is essential for establishing proper spraying swath and buffer zones when spraying near environmentally sensitive area.

ACKNOWLEDGMENT

M.M. Sidahmed acknowledges the support of the American University of Beirut (University Research Board, URB), Beirut, Lebanon, in the form of a Faculty Development Grant.

REFERENCES

ASAE. 2002. Standard S327.2. Terminology and definitions for agricultural chemical application. In *ASAE Standards 2002*, 49th edition, 180. St. Joseph, MI: ASAE.

Brown, R.B. and M.M. Sidahmed. 2001. Simulation of spray dispersal and deposition from a forestry airblast sprayer - Part II: Droplet trajectory model. *Transactions of the ASAE* 44(1):11-17

Desrochers, L. and J. Dunnigan. 1991. Mobile sprayers for ground application of herbicides. Special Report No SR-79. Pointe Claire, QC: Forest Engineering Research Institute of Canada (FERIC).

Hale, O.D. 1975. Development of a wind tunnel model technique for orchard spray application research. *Journal of Agricultural Engineering Research* 20:303-317.

Hale, O.D. 1978. Performance of air jets in relation to orchard sprayers. *Journal of Agricultural Engineering Research* 23(1):1-16.

Legg, B.J., and P.C.H. Miller. 1990. Drift assessment using measurements and mathematical models. ASAE Paper No. 901593. St. Joseph, MI: ASAE.

Miller, J.H. and R.J. Mitchell. 1990. *A Manual on Ground Applications of Forestry Herbicides*. Management Bulletin No. R8-MB-21. Auburn, AL: USDA Forest Services, Southern Forest Experimental Station, Auburn University.

Reichard, D.L., H. Zhu, R.D. Fox and R.D. Brazee. 1992a. Wind tunnel evaluation of a computer program to model spray drift. *Transactions of the ASAE* 35(3):755-758.

Reichard, D.L., H. Zhu, R.D. Fox and R.D. Brazee. 1992b. Computer simulation of variables that influence spray drift. *Transactions of the ASAE* 35(5):1402-1407.

Sidahmed, M.M. and R.B. Brown. 2001. Simulation of spray dispersal and deposition from a forestry airblast sprayer - Part I: Airjet model. *Transactions of the ASAE* 44(1):5-10.

USDA. 1984. Measurement of droplet size frequency from nozzles used for aerial applications of pesticides in forests. Equipment Development Center Report 8434 2803. Missoula, MT: United States Department of Agriculture, Forest Service.

Weiner, K.L., and C.S. Parkin. 1993. The use of computational fluid dynamics code for modeling sprays from a mist blower. *Journal of Agricultural Engineering Research* 55(4):313-324.

Zhu, H., D.L. Reichard, R.D. Fox, R.D. Brazee and H.E. Ozkan. 1994. Simulation of drift of discrete sizes of water droplets from field sprayers. *Transactions of the ASAE* 37(5):1401-1407.

Zhu, H., D.L. Reichard, R.D. Fox, R.D. Brazee and H.E. Ozkan. 1996. Collection efficiency of spray droplets on vertical targets. *Transactions of the ASAE* 39(2):415-422.

LIST OF SYMBOLS

D Droplet diameter (μm)
D_o Initial droplet diameter (μm)
D_{o1} Initial diameter of largest droplet that crosses X_1 (μm)

D_{o2} Initial diameter of largest droplet that crosses X_2 (μm)
D_{oe} Initial diameter of largest droplet that evaporates to extinction (μm)
D_f Final droplet diameter (μm)
D_{f1} Final diameter of droplet with $D_o=D_{o1}$ (μm)
D_{f2} Final diameter of droplet with $D_o=D_{o2}$ (μm)
H Height above the ground (m)
H_f Final height of droplet above the ground (m)
L_f Final distance of droplet from sprayer outlet (m)
RH Relative humidity of ambient air (%)
T Temperature of ambient air (K)
U Outlet axial velocity of airjet (m/s)
V Initial release velocity of droplet (m/s)
X X-axis or horizontal distance from sprayer outlet (m)
X_1 Boundary ($X=X_1$) separating deposition and particle drift regions (m)
X_2 Boundary ($X=X_2$) separating particle and airborne drift regions (m)
Y Y-axis or lateral distance from airjet axis (m)
Z Z-axis or vertical distance from airjet axis (m)
α Spray angle of nozzle (degrees)
β Angle between the central axis of a nozzle and airjet axis (degrees, +ve counterclockwise)
θ Droplet projection angle (degrees, +ve counterclockwise)